Twins: Device-free Object Tracking using Passive Tags

Jinsong Han, *Member*, *IEEE*, Chen Qian, *Member*, *IEEE*, Xing Wang, *Student Member*, *IEEE*, Dan Ma, *Student Member*, *IEEE*, Jizhong Zhao, *Member*, *IEEE*, Wei Xi, *Member*, *IEEE*, Zhiping Jiang, *Student Member*, *IEEE*, and Zhi Wang, *Member*, *IEEE*

Abstract—Device-free object tracking provides a promising solution for many localization and tracking systems to monitor non-cooperative objects, such as intruders, which do not carry any transceiver. However, existing device-free solutions mainly use special sensors or active RFID tags, which are much more expensive compared to passive tags. In this paper, we propose a novel motion detection and tracking method using passive RFID tags, named Twins. The method leverages a newly observed phenomenon called critical state caused by interference among passive tags. We contribute to both theory and practice of this phenomenon by presenting a new interference model that precisely explains it and using extensive experiments to validate it. We design a practical Twins based intrusion detection system and implement a real prototype by commercial off-the-shelf RFID reader and tags. Experimental results show that Twins is effective in detecting the moving object, with very low location errors of 0.75m in average (with a deployment spacing of 0.6m).

Index Terms—Device-free, Passive RFID tag, Tracking, Critical State

I. Introduction

Preventing illegal or unauthorized access of intruders is of importance to protect the security of people, organizations, and their properties. For anti-intrusion purpose, there is an essential need to deploy security systems supported by localization and motion-detecting methods. To this end, existing work performs motion detection using various sensors including passive infrared (PIR) sensors, sonic sensors, and video camera sensors. Those methods, though being able to achieve high accuracy and sensitivity, are not cost-efficient for large scale logistic systems, such as retailing, warehouse, cargo transportation. In recent years, Radio Frequency Identification (RFID) tags have been widely deployed in modern logistic and inventory systems for efficient identification and monitoring. Compared with deploying sensor systems [10, 32], motion detection using RFID tags for anti-intrusion purpose has two main advantages: low cost devices and reuse of existing RFID infrastructure.

Motion detection or trajectory tracking by RFID tags has been proposed in the literature [1-7]. There are two major categories in previous work, device-based and device-free methods. By attaching a tag to an item, the device-based method can identify the location of this item when the tag is interrogated by the reader. However, it is impossible to bind tags to uncooperative objects, such as the intruders. Thus device-based methods are not suitable for intrusion detection and tracking in many practical applications. Device-free solutions are promising to track intruders while keeping them unaware of detection [8].

Most existing device-free object tracking solutions based on RFID systems rely on active tags [3, 7, 8, 28]. However, active tags are much more expensive than passive tags and are less ubiquitous in current deployments. To our knowledge, there is no solution in the literature that can achieve accurate and reliable device-free motion detection with passive RFID tags.

In this paper, we present the first device-free object tracking system using passive RFID tags, named *Twins*. Our method is motivated from a newly observed phenomenon due to the coupling effect among passive tags. Suppose we put the antennas of two passive tags close and parallel to one another, as illustrated in Fig.1. Within a certain distance, the two adjacent tags will present such a phenomenon that one of them, e.g. tag *B* in the left subfigure of Fig.1, just becomes unreadable, due to the coupling effect. It is like that tag *A* casts a "shadow" to tag *B*. As a result, the signal strength of RF waves sent from the reader is significantly reduced at *B*'s antenna. Thus tag *B* cannot receive sufficient energy to perform the computation or modulation, and cannot response to the reader. We name such a situation as *critical state* and such a pair of tags as *Twins* or *a Twin pair* here after.

We then utilize this phenomenon to achieve device-free object tracking. The key insight is to create a critical state of two tags as Twins. If an object or human being moves close to the Twins, as shown in the right subfigure of Fig.1, some RF waves will be reflected or refracted to the Twins, similar to the multipath effect. In this case, the unreadable tag can receive sufficient energy to break the critical state and then become readable. We call this change as a *state jumping*. State jumping infers a nearby moving object.

However, existing interference models of RFID tags contradict to our observations from real experiments and

- *Jinsong Han, Xing Wang, Dan Ma, Jizhong Zhao, Wei Xi, and Zhiping Jiang are with the School of Electronic and Information Engineering, Xi'an Jiaotong University, China. (e-mail: {hanjinsong, zjz, xiwei}@mail.xjtu.edu.cn, { gggjtg, xjtumd, zhiping}@stu.xjtu.edu.cn)*
- *Zhi Wang is with the School of Software Engineering, Xi'an Jiaotong University, China. (e-mail: zhiwang@mail.xjtu.edu.cn)*
- *Chen Qian is with the Department of Computer Science, University of Kentucky, Lexington, Ky. (e-mail: qian@cs.uky.edu)*

cannot explain the critical state phenomenon of Twins. It is because they are "structure-oblivious" models without considering the structure of antenna circuit.

In this work, we develop a novel "structure-aware" interference model of RFID tags based on analysis of the T-match circuit structure [11], which plays an important role in the interaction between two adjacent tags. Comprehensive

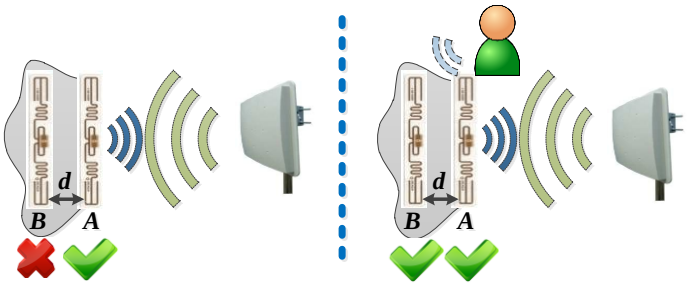

Fig. 1. Critical state of Twins. Left figure shows Tag B cannot be read due to the coupling effect. Right figure shows when an object comes, Tag B becomes readable.

experimental results agree the proposed model and validate the occurrence of the critical state.

We further design a tracking scheme to achieve accurate trajectory monitoring for moving objects. Our scheme employs a combination of a k-nearest-neighbor (KNN) based algorithm and a particle filter based algorithm to approximate the trajectory of intruders. We summarize the major contributions and results of our work as below.

1) We are the first to propose to use critical state of passive tags for intrusion detection and trajectory tracking. By reusing the existing RFID infrastructure, this method is a cost-efficient and accurate anti-intrusion solution.

2) We contribute to the theory of the tag interference model and develop a "structure-aware" model which perfectly explains the critical state phenomenon.

3) We conduct extensive experiments on a real RFID system for validating the feasibility of using critical states for motion detection.

4) We design a tracking method for effective intruder detection and tracking. We have implemented it in a real RFID system using off-the-shelf reader and tags. The experimental results show that our solution can achieve high detection accuracy, i.e. the localization error is 0.75m in average.

II. Background

As the most representative technology of "untouchable" identification, RFID shows many advantages over the conventional labeling techniques. RFID tags can be automatically and remotely interrogated in a non-line-of-sight way. Current RFID tags fall into two categories, active and passive tags. With on board batteries, active tags have a larger communication region and more powerful computation capacity than passive tags, while suffering from much higher manufacture and energy cost. Passive tags are more cost-efficient and battery-free due to simple circuitries.

A. Near-field and Far-field

In RFID systems, the reader and tags communicate via their antennas. The communication patterns include near-field and far-field communications. The boundary between near-field and far-field is determined by the Rayleigh length [12], calculated as $R = 2D^2/\lambda$, where D is the size of antenna and λ is the wavelength of antenna. Equivalently, D is the diameter of the smallest sphere enclosing the antenna. Passive tags are identified by using the far-field communication. According to FCC regulation, passive tags should operate in a spectrum of 902~928 MHz in US. With far-field links, RFID reader interrogates the tag by emitting RF waves, while the passive tag modulates its data into the wave reflected to the reader. This pattern is referred as *Backscatter* communication [11]. On the other hand, the interference between two adjacent tags takes the *coupling effect* in near-field.

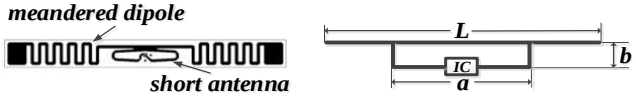

Fig.2. Real tag model and T-match structure.

B. Dipoles and T-match structure

Most passive tags use a half-wave dipole antenna. We show a commercial passive tag, Impinj E-41b in Fig.2. The length of antenna should be $\lambda/2$, i.e. 16cm for 915MHz. To reduce the physical size, the antenna is bent to form a *meandered dipole*. However, meandered dipole faces a problem of matching. A large mismatch of antenna to IC may result in a small power transfer coefficient, and hence a small portion of received power to be used by the tag. One practical treatment for improving the match is to adapt a short antenna to the capacitive IC load, forming a T-match structure, as shown in Fig.2. In this structure, the impedance of the longer meandered dipole (with the length of L) can be tuned by the introduced shorter dipole (with the length of a). The IC of the tag connects to the meandered dipole via two wings of the short dipole.

III. Critical State of Coupling RFID Tags

In this section, we first show a contradiction between the conclusion derived from conventional "structure-oblivious" model and the results observed from real experiments. To address the contradiction, we propose a hypothesis that cannot be explained by the conventional method. We then develop a "structure-aware" model for explaining the interaction of Twins. The model is theoretically proved and perfectly matching the experiment results.

A. Structure free model for coupling tags

In near-field communication, the interaction between two tag antennas is known as *inductive coupling* [12]. Theoretically, the antenna of a given tag can be replaced by an equivalent circular loop [13], which is a common and simple equivalent method. Here, the circular loop is not related to the specific structure of tags. Two nearby tags can be modeled by two

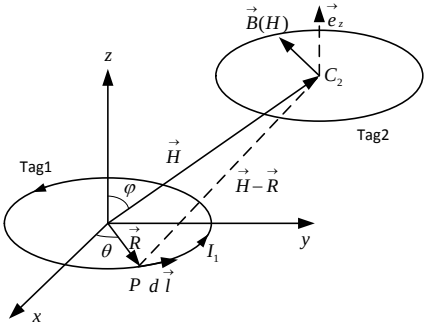

Fig. 3. A structure-oblivious model of two coupling tags.

circular loops as shown in Fig. 3 and in this coordinate system, the center positions of Tag 1 and Tag 2 are (0, 0, 0) and (0, *Hsinφ*, *Hcosφ*), where $\vec{H}$ is the vector from center of Tag 1 to the center of Tag 2 and φ is the angle between *Z* axis and $\vec{H}$.

According to the *Biot-Savart* Law [12] a steady current I_1 at a position *P* on the circular of Tag 1 can generate a magnetic field B_2 on Tag 2:

$$B_2 = \frac{\mu_0}{4\pi}\int_0^{2\pi}\frac{I_1 d\vec{l}\times(\vec{H}-\vec{R})}{\left|\vec{H}-\vec{R}\right|^3}d\theta \tag{1}$$

where μ_0 is the magnetic constant, $d\vec{l}$ is a vector whose magnit ude is the length of the differential element of the wire in the di rection of conventional current, $\vec{R}$ is the radius vector along the angle θ, and $\vec{H}-\vec{R}$ is the positional vector starting from the c urrent segment on the Tag 1's antenna loop and pointing to the center of Tag 2's loop.

Here we introduce the concept of the *mutual inductance M*, which is a measure of the coupling between two indicators. Let $\Psi_{21}(I_1)$ denote the magnetic flux through Tag 2's loop due to the current in Tag 1. Then the mutual inductance M_{21} can be written as

$$M_{21} = \frac{\Psi_{21}(\mathrm{I}_1)}{I_1} \tag{2}$$

According to the magnetic flux definition, M_{21} has the form:

$$M_{21} = \frac{B_2 A_2}{I_1} \tag{3}$$

Here A_2 represents the area of the Tag 2's loop surface where the magnetic field passing through. Applying Equation 1 to Equation 3, the mutual inductance M_{21} can be written as:

$$M_{21} = \frac{\mu_0 A_2}{4\pi}\int_0^{2\pi}\frac{d\vec{l}\times(\vec{H}-\vec{R})}{\left|\vec{H}-\vec{R}\right|^3}d\theta \tag{4}$$

The induced current I_{H_2} in Tag 2 can be calculated from an equivalent RCL circuit of the tag. As the Lenz law [12] indicates, this induced current (I_{H_2}) is so directed as to oppose the change in flux, which has an opposite direction of I_1:

$$I_{H_2} = \frac{-j\omega M_{21} I_1}{R_{chip} + 1/\, j\omega C + j\omega L} = -bM_{21} I_1 \tag{5}$$

where R_{chip}, *C*, *L* are the chip impedance, capacitance, and inductive impedance of Tag 1, respectively. As Tag 1 and Tag 2 are two tags from the same model, we let *b* denote the hardware–relative part of Equation above.

Let I_{01} and I_{02} represent the currents of Tag 1 and Tag 2 generated by harvesting the RF signals from the reader. Then the current in Tag 2 can be represented as $I_2 = I_{02} - bM_{21}I_1$. Analogously, the current in Tag 2 can also generate induced current in Tag 1, which means there exists another mutual inductance M_{12}. Using the *Reciprocity Theorem* which combines the Ampere's law and Biot-Savart law [12], the two mutual inductances are equal, $M = M_{12} = M_{21}$. For the current in Tag 1, we also have $I_1 = I_{01} - bM_{12}I_2$.

In this model, the distance between Tag 1 and Tag 2 is measured by millimeters. Comparing with the longer distance from the reader's antenna to the Twins, e.g. 1 m – 6 m, the two tags can be viewed as in same distance from the reader's antenna. This means for the two tags, the currents I_{01} and I_{02} have an equal direction and value. Therefore, we can get the conclusion of $I_1 = I_2$.

As aforementioned, when two tags are placed very close to each other, the inductive coupling effect will reduce the current in both tag antennas. Meanwhile, following this "structure-oblivious" model, the effects on both antennas are equivalent, which means Tag 1 and Tag 2 will get the same amount of energy to activate their chips. Therefore, they should become both readable or both unreadable simultaneously. However, it contradicts to the observations from our real experiments.

B. Observations from experiments of adjacent tags

We conduct a set of experiments using 20 off-the-shelf tags (Impinj E41-b). We randomly label these 20 tags by A_1, A_2, …, A_{10}, B_1, B_2, …, B_{10} and then form 10 sets of Twins (A_1, B_1), …, (A_{10}, B_{10}). We place the Twins in a plastic foam board. For different pairs of Twins, we change the placement of two tags and record the minimum power needed for reading them, as shown in Fig.4. In these experiments, the distance between two tags is fixed to 10mm, and the distance between tags and the reader's antenna is fixed to 2m.

Since increasing the transmission power of the reader can increase the coupled current in tags, *the minimum power value reflects the scale of current to activate a tag*. For each sub-figure, we simplify the geometry shape of tags for illustrating their relative positions. We define the tag with its IC as the closest part to another tag than its other parts as the *Rear-tag* in Twins, like Tag A in Fig.4 (a). Correspondingly, Tag B will be the *Fore*-tag in Fig.4 (a). The average minimum powers for each tag are shown with bar chart of Fig.4. In Fig.4 (a) – (d), the difference of minimum power in a Twins is about 10 dbm. In other deployments (Fig.4 (e) - (h)), the two tags' minimum powers are almost the same. The big difference of minimum power in Fig.4 (a) - (d) means there exists the "shadowing" effect that causes critical state of Twins. In addition, we can find that in Twins, the Rear-tag is the "shadowed" one that needs more power to be activated. However, none of existing RFID interference models [13, 14]

can explain the existence of the shadowing effect. Based on these models, the two adjacent tags are modeled as two identical circular loops. Since the two tags are equal in the distance to the reader and deflection angle from the axis of the reader's antenna in our experiments, their currents coupled by the reader's RF signals, I_{01} and I_{02} should be equal $I_{01} = I_{02}$.

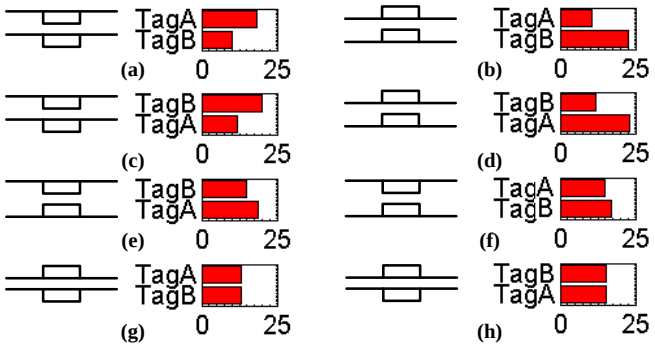

Fig. 4. The placements of Twins and the minimum P_{TX} used for reading them.

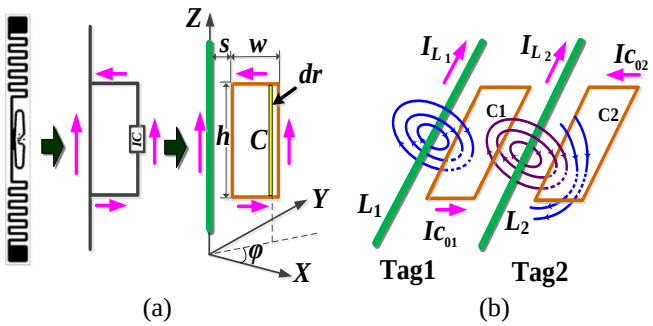

Fig. 5. Structure-aware modeling for the Twins.

Based on the *Reciprocity Theorem* which combines the Ampere's law and *Biot-Savart* law [12], the two mutual inductances are equal, $M = M_{12} = M_{21}$. For the current in Tag 1, we have $I_1 = I_{01} - bM_{12}I_2$, where b is a factor representing the equivalent RCL circuit of the Tag1, which is also equal to that of Tag2. Similarly, we have $I_2 = I_{02} - bM_{21}I_1$. Obviously, $I_1 = I_2$. Here I_1 or I_2 is integrated result of current coupled by the reader's RF signals and the mutual coupling between Tag 1 and Tag 2.

Such a result obviously contradicts our observations from the experiments. It is because these models are "structure-oblivious", meaning they do not consider detailed antenna structure that may cause different interference levels for different placements.

C. Structure-aware model

We introduce a "structure-aware" interference model that can provide reasonable explanation to the phenomenon of shadowing. Instead of using a simple circular loop, we use two dipoles to model the antenna of passive tags, as shown in Fig.5 (a). Note Tag 1 is the Rear-tag. We model the dipole antenna as two components as shown in Fig.5 (a). One is an electric dipole like a line and another is a magnetic dipole like a rectangle. This modeling is well coincident with the T-match structure.

We model Twins as four conductors, two lines (L_1, L_2) and two rectangles (C_1, C_2), shown in Fig.5 (b). Suppose the electromagnetic forces (*emf*) induced by the reader's RF signals in the two lines are $E_{L_{01}}$ and $I_{L_{02}}$, respectively. We have the following proposition.

Proposition: If two tags Tag 1 and Tag 2 are placed as in Fig.5 (b), let E_{C_1} and E_{C_2} be the voltage on C_1 and C_2, respectively, $E_{C_1} < E_{C_2}$.

Proof: As previously indicated in Section III-A, we have $I_{L_1} = I_{L_2} = I_L\ e^{j\omega t}$, where I_L is the complex amplitude. The area of the rectangle is $h \times w$, where the h is the length and w is the width. Let s denote the distance from the rectangle to the line (s is very slight). We assume I_{L_1} and I_{L_2} are in the same direction as Z axis. We analyze the interaction among these four conductors as follows.

1) Mutual inductance between C_1 and C_2

According to *Reciprocity Theorems* [12], C_1 and C_2 is symmetric to each other. The coupled current, denoted as $-I_H$, has an identical value in C_1 and C_2, while the coupled current is always in the opposite direction to the exciting current.

In Fig.5.(b), the coupling effect center of $-I_H$ should be at the geometric axis of C_1 or C_2. According to *Neumann Formula* [12], the magnetic vector, induced by the current I_1 in C_1, can be represented as:

$$A_1 = \frac{\mu_0 I_1}{4\pi}\oint_{C_1}\frac{dC_1}{D} = \frac{\mu_0 I_1 hw}{4\pi d^2} \tag{6}$$

The mutual flux, which is induced by I_1 and linked with C_2 will be

$$\begin{aligned}\Psi_{21} &= \oint_{C_2} A_1 \cdot dC_2 \\ &= \frac{\mu_0 I_1}{4\pi}\oint_{C_2}\oint_{C_1}\frac{dC_2 \cdot dC_1}{d} \\ &= \frac{\mu_0 I_1 hw}{2\pi d^2}(h+w)\end{aligned} \tag{7}$$

Therefore, the mutual inductance between C_1 and C_2 is

$$\begin{aligned}M_{21} = M_{12} &= \frac{\Psi_{21}}{I_1} \\ &= \frac{\mu_0}{4\pi}\oint_{C_2}\oint_{C_1}\frac{dC_2 \cdot dC_1}{d} \\ &= \frac{\mu_0 hw}{2\pi d^2}(h+w)\end{aligned} \tag{8}$$

Since Tag 1 and Tag 2 are in the same model, the area of C_1 is equal to that of C_2. Let C to denote C_1 or C_2. The induced *emf* at C_1 or C_2 is

$$\begin{aligned}E_H &= \frac{d\Psi}{dt} = \frac{MdC}{dt} = j\omega I_L e^{j\omega t}M \\ &= \frac{\mu_0 j\omega I_L e^{j\omega t} hw}{2\pi d^2}(h+w)\end{aligned} \tag{9}$$

2) Mutual Inductance in C_1

The mutual inductance in C_1 is an integration of the mutual inductances between L_1 and C_1, between L_2 and C_1, and between C_1 and C_2.

a) Mutual inductance between L_1 and C_1

The magnetic induction B yielded by current I_{L_1} can be represented as concentric circles around L_1. In the cylindrical model in Fig.5(a), the magnetic induction B in position (r, φ, z) can be calculated by using the *Biot-Savart* Law [12] as

$$\vec{B} = \overrightarrow{e_\varphi}\mu_0 I_{L_1}\frac{1}{2\pi r} \quad (10)$$

where μ_0 is the magnetic constant and $\overrightarrow{e_\varphi}$ is the unit direction vector of the magnetic induction.

The magnetic flux caused by I_{L_1} within the rectangle C_1 can be calculated as the integral from s to $s + w$

$$\Psi_{11} = \int_{C_1}\vec{B}_{C_1}d\vec{C} = \frac{\mu_0 I_{L_1} h}{2\pi}\int_s^{s+w}\frac{1}{r}dr = \frac{1}{2\pi}\mu_0 I_{L_1} h\ln\left(\frac{s+w}{s}\right) \quad (11)$$

where the dr is the tiny rectangle facet primitive within the C_1, Note $d\vec{C} = h*dr$.

As discussed in Equation 2, the mutual inductance M_{11} of L_1 and C_1 is

$$M_{11} = \frac{\Psi_{11}}{I_{L_1}} = \frac{1}{2\pi}\mu_0 h\ln\left(\frac{s+w}{s}\right) \quad (12)$$

The induced electromotive force in C_1 is

$$E_{f_1} = -\frac{d\Psi_{11}}{dt} = -\frac{M_{11}dI_{L_1}}{dt} = -\frac{\mu_0 hj\omega I_{L_1}e^{j\omega t}}{2\pi}\ln\left(\frac{s+w}{s}\right) \quad (13)$$

Since the magnetic flux of L_1 is in an opposite direction with that of C_1, the two opposing magnetic fluxes have a force of canceling out to each other. Thus, the induced electromotive force in C_1 is negative: $E_{11} = -E_{f_1}$.

b) Mutual inductance between L_2 and C_1

The coupling effect between L_2 and C_1 can be derived similarly. The mutual inductance can be written as

$$M_{21} = \frac{\varphi_{21}}{I_{L_2}} = \frac{1}{2\pi}\mu_0 h\ln\left(\frac{d+w}{d}\right) \quad (14)$$

On the other hand, the direction of magnetic flux of I_{L_2} is the same as that of C_1, the integrated magnetic flux is enhanced. We have

$$E_{21} = \frac{\mu_0 hj\omega I_{L_2}e^{j\omega t}}{2\pi}\ln\left(\frac{s+w}{s}\right) \quad (15)$$

3) Mutual Inductance in C_2

Similar to Equation 13 and 15, we can calculate the coupling effect between L_1 and C_2, and the coupling effect between L_2 and C_2, which are denoted as E_{12} and E_{22}.

$$E_{12} = \frac{\mu_0 hj\omega I_{L_1}e^{j\omega t}}{2\pi}\ln\frac{2s+2w+2d}{2s+w+d} \quad (16)$$

$$E_{22} = \frac{\mu_0 hj\omega I_{L_2}e^{j\omega t}}{2\pi}\ln\left(\frac{s+w}{s}\right) \quad (17)$$

4) Voltage in C_1 and C_2

Suppose E_{C_1} and E_{C_2} are the induced *emf* in C_1 and C_2 generated by harvesting the RF signals from the reader's antenna. Since the induced currents $I_{L_1} = I_{L_2}$, we denote N as

$$N = \frac{\mu_0 hj\omega I_{L_1}e^{j\omega t}}{2\pi} = \frac{\mu_0 hj\omega I_{L_2}e^{j\omega t}}{2\pi}$$

Then we can get the representation of E_{C_1} and E_{C_2} as:

$$E_{C_1} = E_{C_{01}} + E_{11} + E_{21} - E_H = E_{C_{01}} + N\ln\frac{s+w}{s} - N\ln\frac{d+w}{d} - \frac{Nw}{d^2}(h+w) \quad (18)$$

$$E_{C_2} = E_{C_{02}} + E_{12} + E_{22} - E_H = E_{C_{02}} + N\ln\frac{2s+2w+d}{2s+w+d} - N\ln\frac{s+w}{s} - \frac{Nw}{d^2}(h+w) \quad (19)$$

We know that $E_{C_{01}} = E_{C_{02}}$ from the analysis using the "structure-oblivious" model. Thus, $E_{C_2} > E_{C_1}$. ■

Here we consider the impact from D, *i.e.*, the distance between two tags. For two given tags, *i.e.*, given the s, w, h are fixed for the two tags, if varying D, we rewrite E_{C_1} and E_{C_2} as $E_{C_1} = E_{C_{01}} + \Delta E_1$ and $E_{C_2} = E_{C_{02}} + \Delta E_2$.

Case1. d is sufficient large, $d \gg w$.

Considering that

$$\lim_{\frac{w}{d}\to 0}\left(\frac{d+w}{d}\right) = 1 \qquad \lim_{\frac{w}{d}\to 0}\left(\frac{2s+2w+d}{2s+w+d}\right) = 1$$
$$\lim_{\frac{w}{d}\to 0}\left(\ln\frac{d+w}{d}\right) = 0 \qquad \lim_{\frac{w}{d}\to 0}\ln\left(\frac{2s+2w+d}{2s+w+d}\right) = 0$$

and $E_{21} = E_{22}$, $E_{C_1} \approx E_{C_2}$. This indicates that the inductive coupling effect of the two tags is nearly identical to each other, when the distance between two tags is sufficiently large.

Case 2. d is small, *i.e.*, d is scale to the w.

We calculate the derivative of ΔE_1 as follows.

$$f(d) = \frac{Nw}{d}\dot{(}\frac{1}{d+w} + \frac{h+w}{d^2}) > 0 \quad (20)$$

Here $f(d) > 0$ because the value of each element in Equation 20 is positive. Then ΔE_1 is monotonically increasing. In the extreme case of $d = s$, *i.e.*, the distance between two tags is minimized. Then we have

$$\Delta E_1 = -\frac{Nw}{d^2}(h+w) < 0 \quad (21)$$

This means within a certain distance $s + \Delta d$, ΔE_1 always shows a negative value and reduces the value of E_{C_1}. Let E_w be the operation voltage threshold at which the chip of tags can operate. Especially, if $E_{C_{01}} \approx E_w$, $E_{C_{01}} < E_w$ due to the impact of ΔE_1. In this situation, Tag 1 will not have sufficient power for operation, *i.e.*, being unreadable. Note that this is very easy to achieve $E_{C_{01}} \approx E_w$, because $E_{C_{01}}$ will be reduced if enlarging D or decreasing the transmission power of the reader.

On the other hand, $E_{C_2} > E_{C_1}$. It is highly possible that Tag 2 is still readable when Tag 1 JUST becomes unreadable, *i.e.*, $E_{C_{02}} > E_w$.

5) Critical state and state jumping

According to above discussion, when the distance between two adjacent tags d is within the range of $s + \Delta d$, the critical state can be easily triggered to one tag of the Twins. In particular, Case 2 in the previous subsection explicitly explains why the Rear-tag always becomes unreadable in our experiments. This result indicates that the proposed structure-aware model is feasible for explaining the "shadowing" effect in two tags "facing the same" discovered from real experiments, as the examples in the Fig.4 (a) – (d). On the other hand, the state jumping is mainly caused by the extra RF reflected by the moving object. Considering a Twins in Case 2, a critical state occurs at Tag 1. Tag 1 JUST enters such a state, *i.e.*, $E_{C_1} \approx E_w$. In this case, suppose a small portion of extra RF signals, *e.g.*, reflected by the moving person, impinges to Tag 1. It will augment E_{C_1} such that $E_{C_1} > E_w$. As a consequence, Tag 1 can obtain sufficient energy again for

backscattering RF signals to the reader. If the reader receive the signals and identify Tag 1, it becomes readable, yielding a state jumping to alert the appearance of a moving object.

IV. Validation of the State Jumping Phenomena

In this section, we experimentally validate the critical state and state jumping phenomena. First, we deploy two tags A and B as Twins and a reader as shown in Fig.6. We then create a critical state of the Twins by tuning the transmission power of the reader, P_{TX}. To enable a fine-grained tuning, we employ a UI of Impinj readers, named MultiReader. In this phase, we first set P_{TX} to 32.5 dBm, and then gradually decrease P_{TX}. For each step, the reader attempts to interrogate the Twins. A critical state occurs if one tag becomes unreadable.

Let d denote the distance between two tags, and D denote the distance from the reader to the Twins. We vary d from 6 mm to 26 mm and try to yield a critical state for the Twins with a fixed D of 2 m. We find that a critical state occurs when the distance is less than 15 mm as shown in Fig.7. Tag B, which is the Rear-tag in the Twins, is always the one that cannot be read in the critical state. Tag B shows a higher minimum value of P_{TX} than that of Tag A. When d decreases, the difference between values of P_{TX} of the two tags becomes larger.

In the next phase, a volunteer moves around the Twins to determine the regions where critical state happens. As Fig.10. shown, the object always appears in the sensing area from far to near. The state jumping occurs when the object moves close to the line between a reader and twins. Under this situation, the object will first reflect more signals before blocking the line-of-sight signals. The "in-between" deployment pattern is motivated by two reasons.

First, the propagation feature suggests the in-between instead of 'behind' deployment pattern. In passive UHF RFID systems, the electric and magnetic fields propagate as the RF wave, which is indeed an electromagnetic (EM) wave. Since the UHF RFID system works in far field, in which the form of electromagnetic radiation is only the radiative coupling. According to the propagation law of such EM waves, *i.e.*, Free space model, the EM field decreases by a factor of $1/R^2$, where R is distance between the tag and reader antenna. Thus, the signals reflected from a 'in-between' person will be more powerful that reflected from a 'behind' person. This indicates that Twins will be more sensitive to those objects between it and the reader's antenna. Meanwhile, each reflection or refraction of the human body will increase the path loss. That is, the 'behind' deployment pattern impinge much weaker signals than in-between deployment pattern, and hence is with much smaller probability to trigger a state jumping.

Second, the 'in-between' deployment pattern is more suitable for the real logistics or retailing application, where many shelves are arranged in rows and there are some aisles between two shelves. For better detecting the moving person in the aisle, it is intuitive to adopt the 'in-between' deployment. If adopting the 'behind' pattern, the blocking effect of the shelf and the items in the shelf will degrade the detection performance of Twins.

We record the occurrence of state jumping caused by the moving volunteer and show the corresponding positions in Fig.8. We divide the experiment area into small cells, and count the number of state jumping events in each cell.

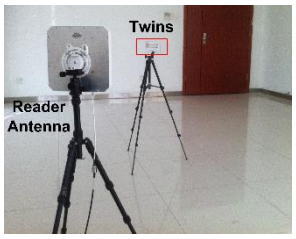

Fig. 6. Validation setup.

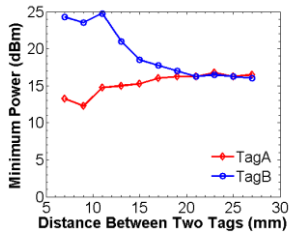

Fig. 7. Minimum P_{TX} vs. d.

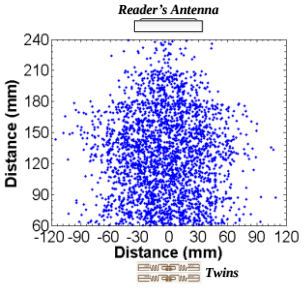

Fig. 8. # of state jumping.

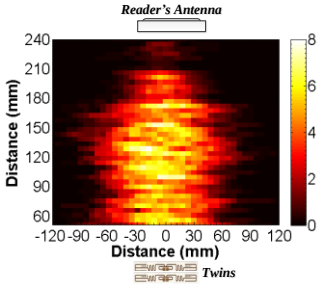

Fig. 9. Effective region.

The results are plotted in Fig.9. This figure geometrically illustrates the sensitivity of detecting moving objects. It can be found that the effective range of detection is relatively large, about a 2 m × 1 m rectangle between the reader and Twins. When the volunteer moves behind the Twins, the effective range of detection is reduced to 1m away from the Twins.

V. Tracking Moving Objects Using Critical State

We employ a combined methods for device-free object tracking. The *minimum connected component based method* is used for object localization, and the particle filter [15] is used for tracking the object trajectory. Localization is the basis for tracking, so we combine these two methods in our object tracking system and experiments. Note that we focus on tracking a single object in this paper and leave multiple-object tracking in future work.

A number of Twins are deployed in the given area, which could be, for instance, the alleyway between two shelves with valuable items. We assume each pair of Twins is fully covered by at least one reader's interrogation range. The entire region is partitioned into a 2D grid, as shown in Fig.10. In practice, the distance between two pairs of Twins, i.e., the length of cells edges, can be determined based on measurement results. We can formulate the grid as a graph $G = <V, E>$, where each cell in the grid is a vertex in G, and two adjacent cells have an edge in G. If state jumping is detected at Twin pairs, the corresponding cells will be highlighted as shown in Fig.10.

A. Identifying state jumping

When an object moves in the monitored region, it triggers a serial of state jumping events on multiple Twin pairs. Timely outlining the regions including these Twin pairs is essential to track the object movement. However, there remains a challenging issue. At any time, the reader can only have a fixed value of transmission power P_{TX}. Therefore the reader can only

create the critical state for one Twin pair at the same time. Intuitively, the reader can iteratively and sequential queries all

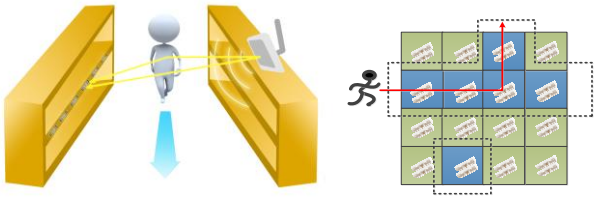

Fig. 10. Intruder detection in warehouse.

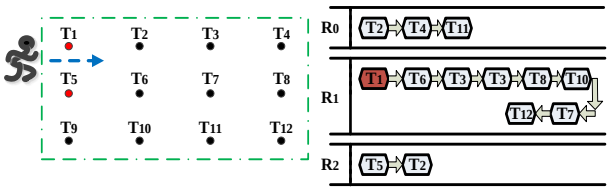

Fig. 11. Example of moving object tracking

Twin pairs within its detection region. However, sequentially query may miss potential state jumpings, if the movement is so fast that the object has moved out of the cells when the Twin pairs are queried. Using a more sophisticated strategy, the reader can preferentially query the nearby Twin pairs of the Twins that just had a state jumping. However, scheduling starvation may occur on some Twin pairs if they have low priority in such scheduling.

To deal with this problem, we propose a simple polling algorithm to achieve timely and efficient movement detection without introducing starvation. According to the datasheet, the Impinj R420 reader can support a 340 times/s interrogation rate. However, following EPC Class 1 Gen 2 specification, the backscattered signals from passive RFID tags may collide with each other. Hence, when the number of tags increases, the interrogation rate would decrease because of collisions. In our prototype system, which area is in a size of 30 m × 20 m, there are 72 Twins pairs, *i.e.*, about 144 tags. It is hard to inventory all these tags within 1s. Fortunately, in a real scenario, an

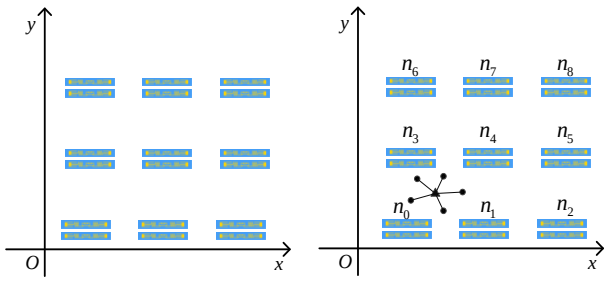

(a) Initial status of the Twins grid (b) an object is in the area

Fig.12. Particle filter.

intruder may move at the speed of 1m/s, or up to 5 m/s. That means an underlying interrogation area up to about 79 m^2. Therefore, we only need to probe the tags within such an area, *i.e.*, about 20 tags. It is easy to inventory all of 20 tags within 1s. Given N Twin pairs in the system, the objective of the polling algorithm is to find a set J of Twin pairs with state jumping caused by object movement within a short time interval.

We use the following data structure in our algorithm. For the ith Twin pair in the graph G, we store a tuple $t_i = <T, P_{TX}, P, S>$ in the database, where T denotes the ID number of the Twins, P_{TX} denotes the corresponding transmission power of reader's antenna to create the critical state for the Twins. P and S are two bits representing the query priority and access status of the Twins. If $P = 1$, which means the Twins is more likely to have a state jumping, then it has a high priority to be queried. Bit S indicates whether the Twins has been accessed in a polling round and hence we can avoid unnecessary queries.

The polling algorithm is iteratively conducted through rounds of queries of the Twins whose P is 1. The idea behind our polling algorithm is that if a Twin pair is experiencing a state jumping, its neighboring Twins are most likely to be triggered by the object movement to a state jumping. Thus, those Twin pairs should be set with a high priority to be queried. We construct a linked list L to order such Twins. If this list is empty, the system will randomly choose some Twin pairs and move their neighboring Twin pairs to list L in the next round. Such a treatment can address the "cold start" problem.

Figure 11 shows an example of our algorithm. At the beginning, we randomly select Twin pairs T_2, T_4 and T_{11} in the polling round R_0. Before starting the next round R_1, we set the bit S to 0 for all Twin pairs in database. Then, we replace each Twins in L with their neighboring Twin pairs, e.g. replacing T_2 with T_1, T_6, and T_3. As a result, in the round R_1, the Twins in list L are [T_1, T_6, T_3, T_3, T_8, T_{10}, T_7, T_{12}] and their priority bit P are set to 1. During round R_1, we sequentially access the tuple of Twins in L. For each Twin pair in the list, we will check whether its S is zero. If $S = 0$, which means this Twin pair is unvisited, we query this Twins by setting the transmit power of reader to its P_{TX}. If it is experiencing a state jumping, we will keep it in L. For any Twins removed from L, we set its $P = 0$. For the example in Fig.11, suppose that in R_1, Twins T_1 and T_5 are trigged due to the moving object. Therefore, T_1 will stay in the list while T_6 and T_3 will be removed, while their P is set as 0. At the end of each query on a pair of Twins, we will set its $S = 1$ to indicate that these Twins pairs have just been checked in this round. For instance, the second T_3 in L will be removed from L when it is checked in R_1. We check all Twins in L using above rules in each round. At the end of R_1, only T_1 is retained and its neighboring pairs T_2, T_5 are selected to be removed in L in the next round.

In short, the algorithm can identify all Twin pairs having state jumping in a short time interval with high probability. These Twin pairs along with the timestamps of the queries will be used for drawing a region where the object most likely stays.

B. Localizing an object

Based on the detected state jumping on Twins, we can outline the region where the object stays.

Ideally, the region should be represented by a connected subgraph G_s in G. However, the movement of an object may render several subgraphs unconnected in G, due to the multi-path effect or ambient noise. We show an example of two separate regions in Fig.12. In this case, we simply select the

largest subgraph in G, termed as G_s and filter other disconnected ones out. If there are more than two subgraphs, G_s is set to the minimum connected component in G that includes all subgraphs.

After determining the possible region that the object stays, we estimate the current position of the object by calculating the centroid of the positions of all Twins in this region. Suppose there are k Twin pairs in the region whose positions are $X_1, X_2,.., X_k$, respectively. The estimated position is C = $(X_1 + X_2 + \ldots + X_k)/k$. We evaluate the tracking accuracy in Section VII.

C. Tracking the object based on improved particle filter

A particle filter is designed to optimize the estimation for non-linear and non-Gaussian state-space models. The main principle of particle filter is to introduce a group of "particles", which actually are random samples in the state space. Utilizing those particles, the distribution of a latent variable can be "filtered" (approximated) at a specific time, given all observations up to that time. By iteratively filtering and re-sampling, the state of the system or targeted object can be estimated. If the state contains the position or derivatives of the position, we can achieve the trajectory of the object.

Suppose that an object moves into the monitored area. We set the main entrance of the area as the origin of coordinates. In Fig.12, n_0~n_8 represent the times of state jumping at the corresponding Twins in Δt. We define the vector $V = (n_0, n_1, n_2, \ldots, n_8)$ as the *observation*. A particle filter is performed via two-phase, offline training and online detecting.

In offline training phase, we estimate the marginal distribution of n_i and the position of object l $P(n_1, n_2, \ldots, n_N | l) = \prod_{i=1}^{N} P(n_i | l)$. Note that l is known in the offline training phase. The estimation discretizes the distribution P into histogram bins, and forms the fingerprint of the position l.

In online detecting phase, particle filter is conducted by five steps: initialization, prediction, weight computation, resampling and approximation. Since there are a lot of works [16] describing how to perform this process, they won't be covered here.

VI. Discussion

A. Proper detection region

Observed from our experiments, state jumping is much easier to occur if the object sits between the Twins and the reader, instead of being behind the Twins. It is mainly because the object moving behind triggers a weaker disturbance to the RF signals around the Twins than in the "in-between" space. Furthermore, detection becomes much unreliable if the Twins are attached to items. In our prototyping and experiments, we adopt the "in-between" deployment for the reader and Twins.

B. Critical state of a single tag

This subsection explains why we do not use a single tag for the moving detection via its own critical state. That is, the reader can probe using the minimum transmission power that can identify a tag in a given position. If one object moves nearby, the tag may also become readable. We perform the experiment on single tag and find that the single-tag method is, however, much less robust than Twins in controlling critical states. The major difference of Twins based detector and single-tag based detector is two-fold: 1) The critical state of Twins tags provides sufficient detection range and sensitivity. In RFID systems, the reader interrogates the tags by emitting RF signals. After the forward (from the reader to a tag) propagation and backward backscattering (from the tag to the reader), the RF signals returns to the reader and can be used for identifying the tag. In this procedure, multipath effect lead a significant impact on the identification, especially in the indoor environment. Even if the signals from some paths, e.g., the line-of-sight path, are blocked, as the case in this example, the signals from other paths may still be impinged to the tag. As a result, the shift from a readable state to unreadable state for a tag can only be achieved within a very short distance. This indicates that the single tag's state change is insensitive to the movement of nearby objects. To demonstrate this phenomenon, we conduct new experiments. As shown in Fig. 13, we can find that the single-tag based critical state approach cannot meet the need of sensitive detection on the moving object with a sufficiently long distance. 2) The critical state of Twins tags are much more stable than that of single-tag. We perform experiments on the single tag scenario. The results shows that the single-tag cannot guarantee stable detection on moving object, either missing the object or leading to false alarm. On the contrary, the Twins system has a high detection rate and does not produce false alarm in the experiment. We leave the study of addressing the stability of critical state for a single tag in our future work.

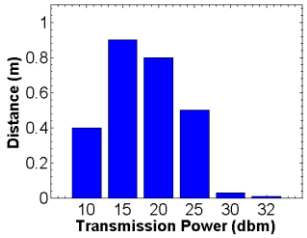

Fig.13. Sensing range of single tag

C. Multiple moving objects

In this work, we focus on tracking a single object. If the area monitored has multiple moving objects, can we still be able to detect them using the Twins method? Indeed, the Twins based tracking scheme has a potential solution. Actually, if there are multiple objects moving in the area, their movements may result multiple subgraphs in G. Intuitively, we can track those objects via those subgraphs. However, there are many challenges in plotting the subsequential trajectories for those objects, considering the scenario that their moving trajectories may cross or overlap. Since tracking multiple objects is out of the scope of this paper, we will give a solution in our future work.

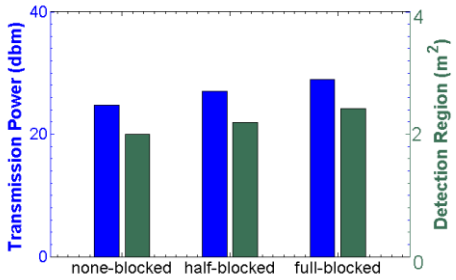

Fig. 14. Impact from environmental changes

D. *Impact from environmental changes*

In the Twins deployment, we need to consider the impact from ambient changes. For example, the shelves used for deploying the Twins can be empty at some time but becomes fully stocked later. The influence of the surrounding obstacles may influence the effective detection region and critical transmission power. Fig. 14 shows the influence of the obstacles on the effective detection region and critical transmission power. In Twins, obstacles have limited impact to the system, if they are static. The reason is that obstacles or a shelf are just a part of environments. Once the Twins is deployed, *i.e.*, entering the critical state, the RF signals reflected from the obstacle or shelf will be unchanged. On the other hand, the state jumping of a Twins is only triggered by the moving object, because the movement may reflect extra RF signals to the Twins. Therefore, the ambient influence to the Twins can be ignored if the surrounding environment keeps static before and after the Twins enters the critical state. The only impact to the Twins is the transmission power required by the reader to generate the critical state for the Twins. If the shelf becomes fully stocked, yielding a critical state for a Twins may need a higher transmission power of the reader. Nevertheless, this is can be easily achieved by tuning the transmission power of the reader. This indicates obstacles have negligible impact on the effectiveness of Twins in detecting moving objects.

E. *System overhead*

The cost would be a major consideration on this work, due to the relatively expensive price of readers and antennas. If we only afford a few of RFID readers, there will be many uncovered regions for a large surveillance area. As a consequence, the system may fail to effectively detect the moving object. We argue that the work is suitable for the logistics scenarios where an RFID infrastructure has been available so that the critical areas will be covered by RFID readers. Nevertheless, the cost is still a challenge. In this case, we can deploy the reader and antenna to cover crucial regions, such as the major entrances or shelves containing valuable items.

When applied to a larger area, we can use multiple antennas to extend the reading range, since the price of antennas of an RFID reader are relatively cheap. The Impinj Speedway R420 reader supports up to 4 antennas. Also, there are other commercial devices helping to push the limit of the number of antennas. As an example, Impinj's Speedway Antenna Hub provides a low cost opportunity to create a large, contiguous RFID read zone with many antennas connected to a single reader. The Speedway Antenna Hub supports up to 32 antennas, which can cover an area larger than 1 km^2, connected to a single Speedway Revolution R420 reader for a robust solution to antenna-intensive RFID applications.

Furthermore, the problem of tracking an object is to identify the sequence of its path segments that is most likely to produce the observed sequence of Twins experiencing a state jumping. There are many effective approaches available to solve above problem, such as the HMM and Viterbi decoding used in [2]. We will address this problem in our ongoing work.

VII. Implementation and Evaluation

In this section, we describe the prototype implementation and performance evaluation. We conduct the experiments in two aspects. First, we investigate the performance of critical state creation and detection. Second, we implement a Twins prototype and conduct comprehensive experiments to evaluate the effectiveness and efficiency of object tracking.

A. *Hardware*

Figure 13 shows the key hardware components in our prototype. The hardware is entirely built from current commercial products and requires no modification on both the reader and tag sides. The reader is an Impinj Speedway R420,

Fig. 15. Experiment hardware

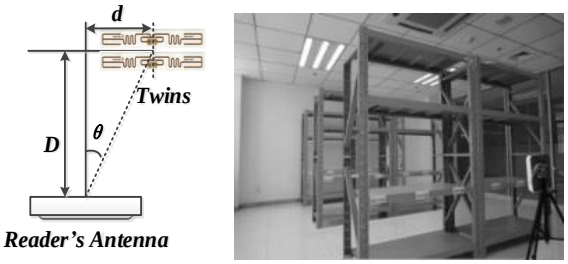

(a) Calibration experiment (b) Prototype system

Fig.16. Experiment setup.

using the EPCglobal UHF Class 1 Gen 2/ISO 18000-6C air protocol. The reader antenna operates in a spectrum of 920~928MHz. The transmission power ranges from 10 to 32.5 dBm. We use 500 E41-b tags in our experiments. E41-b is a widely-deployed off-the-shelf passive tag from Impinj.

B. *Methodology*

1) *Calibration*

The goal of calibration is to determine the proper settings of Twins for motion detection. We investigate the performance of a Twin pair in detecting moving objects nearby. As shown in Fig.14 (a), we find proper values for distance d and angle θ between the antennas of Twins and the reader, distance between the Twins and moving object, and height from the Twins to the floor h.

2) *Prototype*

In the experiment, we implement our prototype system for the surveillance in a warehouse. We setup a testbed with a number of real shelves aligned as shown in Fig.14 (b). Each Twins is attached to the shelf. The distance between two shelves is 2 m. A volunteer walks among the shelves. In the offline training phase, the distance between two adjacent locations where the volunteer stands is 0.6m, since the Twins pair is spaced by 0.6m. We examine the performance of detection rate and probe the proper settings for practical deployment.

3) Experiment environment

We run experiments in a large warehouse to evaluate the tracking accuracy of Twins. The area is in a size of 30m×20m and deployed with Twins grid. The height of the intruder is 1.70m and the moving speed is 1.5 m/s.

C. Performance Evaluation

1) Key parameters of Twins

Through extensive calibration, we investigate the crucial settings in the creation of critical state. We evaluate the impact of different factors on the successful detection rate *r* of the moving object in the monitoring region.

The main lobe width of the reader's antenna used in the prototype is 70°. Thus, it is not necessary to set a θ larger than 35°. We exam the value of *r* by varying θ as 0°, 15° and 30°. For each value of θ, we vary the distance *D* by 75 cm, 105 cm, 135 cm, and 165 cm. With each value of *D*, we set the distance *d* as 6 mm, 8 mm, 10 mm, 12 mm, and 15 mm. Therefore, we have 3*4*5 = 60 test cases. For each case, we conduct 100 runs of experiments. The result is summarized in Fig.15. The X axis contains different settings of *d*. The Y axis represents the detection rate *r*. We differentiate the settings of angle with different colors. We have an observation that setting d = 10 mm can result in the maximum *r* in most cases. We then adopt a default setting of *d* as 10 mm in the following experiments.

We invite three volunteers to play the role of intruders and walk among the shelves in our prototype. The three volunteers are 160 cm, 170 cm, and 180 cm in height, respectively. Their average walking speed is 1.5 m/s. The results are reported in Fig.16. We find that the system has a higher detection rate on taller persons. The reason is that the taller person has a larger cross-sectional area such that more RF waves can be reflected to the Twins, yielding a state jumping with higher probability. We also notice that the detection rate is always over 80% for all volunteers, and 90% for the volunteers with a 1.70+ m height. This result shows that our system is relatively height-insensitive in detecting human movements. Our system is also feasible when changing the distance between Twins and reader antenna *D*. We vary the value of *D* and exam the transmission power P_{TX} to drive the Twins into the critical state. According to Fig.17, we find that a larger *D* requires a higher P_{TX}. Therefore, the maximum deployment distance of Twins depends on the maximum transmission power of reader, e.g. 5.8 m when P_{TX} = 32.5 dbm if using the Impinj R420 reader.

We then probe a proper setting on the height of Twins above the floor in real deployment. Let *h* to denote this value. Figure 18 shows the successful detection rate with different settings of *h*. The X axis in Fig.18 represents the distance between the volunteer and Twins. We notice that when *h* equals to 75 cm, Twins can achieve the highest detection rate (95.17% in average). This is because when *h* = 75 cm, the movement of arms and legs helps to reflect more RF signals to the Twins via multipath effects, which is easier to trigger a state jumping. However, when the height of Twins is too low or too high (e.g. 50 cm or 100 cm), the movement leads a smaller impact on the Twins, and results in a lower detection rate.

The distance between two adjacent Twins pairs is another key parameter. We vary the distance from 0.3m to 1.5m, and investigate the position error. We report the result in Fig. 22. We find that the position error is very similar if the two adjacent Twins pairs are spaced by 0.3m and 0.6m, while increasing slightly by 0.9 m. However, the error increases to nearly 1.4m if the spacing distance increases to 1.5 m. As the effective region shown in Fig.8, the area is about 2 m × 1 m. The results imply that if the spacing distance approaches 2 m, fewer Twins pairs capture the object's movement. In contrast, if we reduce the spacing distance, more Twins pairs can detect the object's movement. When the distance is smaller than 0.6 m, the tracking error is still about the 0.75 m. It is because that a reader can only read a certain amount of tags per second due to the existence of tag signal conflict. Too dense deployment of Twins will reduce the system efficiency. According to the result in Fig. 22, we set the default distance of two adjacent Twin pairs as 0.6 m, which enables a balance between the position error and overhead.

2) Tracking accuracy

We investigate the accuracy of Twins-based tracking scheme and compare it with two well-known RFID based device-free approaches, LANDMARC [3] and TASA [7] through experiments. LANDMARC is active tag based and TASA is a hybrid system of active and passive tags. The tags are deployed in a tag array in all three approaches. The distance between the nearest neighbors in a row or column is 1 m for LANDMARC and 0.6 m for TASA.

During the procedure of tracking the simulated intruder, we use the distance from the estimated position to the real position as the localization error for each experiment. The results plotted in Fig.19 exhibit that the Twins method has a better tracking accuracy than both of LANDMARC and TASA in average. Although Twins is not accurate in a small portion of positions on the moving path, its position error rate is always below 0.85 m, which is 0.75 m in average. Note the infrastructure cost of LANDMARC and TASA is much higher than that of Twins.

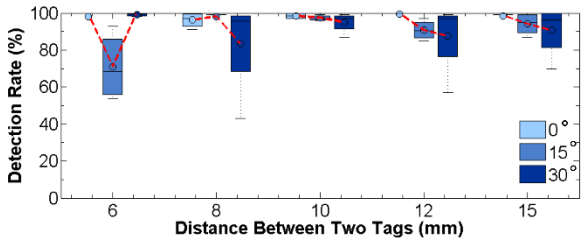

Fig. 17. Calibration result for single Twins.

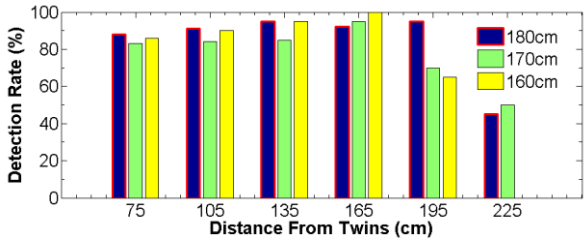

Fig. 18. Impact from the object with different heights.

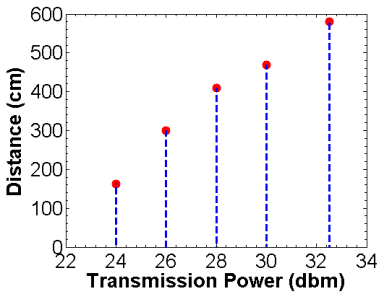

Fig.19. P_{TX} vs. D.

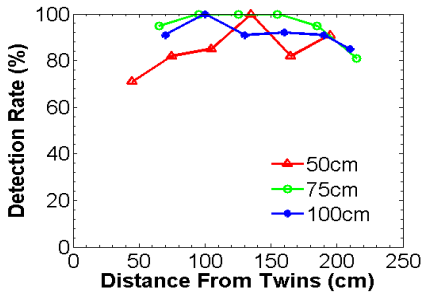

Fig.20. The height above the floor.

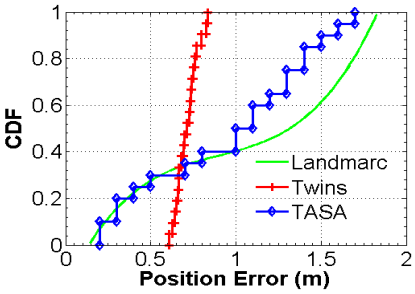

Fig. 21. Tracking accuracy.

VIII. Related Works

The idea of utilizing wireless signals for activity sensing is not new [3]. It continuously attracts attentions recently, due to the prevalence of today's wireless and mobile devices. Research community has proposed many solutions for localizing and tracking objects by using rich sensors [33] and various context attributes, including the GSM [17], WiFi [18, 29, 30], GPS [19], FM [20], and acoustic signal [21, 31]. Prior work in the literature can be categorized into two groups, device-based and device-free approaches. The former category normally requires a device to be bound with the target, while the latter one has no need to bind a device to the target.

Device-based approaches require the target attaching or holding a transceiver. Among those works, LANDMARC [3] is a pioneering work of exploiting the RSS change for localization and tracking. It first site-surveys the RSS-based position fingerprint of a tag-array-covered area. Tracking an active tag can be realized by matching the collected RSS change with the position fingerprint [3]. There is a growing interest in crowdsourcing the sensing capacity of a large amount of computing devices that are held by unprofessional users, such as the works Zee [22] and LiFS [23].

Passive tag based localization is often deployed in the warehouse or library for accurately locating the desired item or book [4, 9, 24, 25]. Choi et al [25] propose a localization algorithm LDTI. LDTI locates the box in a shelf by detecting the tag-interference among the reference tags and target tag. PinIt [24] is one of the most recent works that exploit a passive tag's multipath profile for positioning the object. The work employs the synthetic aperture radar (SAR) imaging mechanism to achieve high accuracy in locating the passive tang. The work shows a promising direction for leveraging multipath effect for localizing low-cost mobile devices.

However, device-based solutions require the desired object to be with a device for localization, which are orthogonal to Twins.

On the other hand, Device-free Passive (DfP) localization is more suitable for monitoring uncooperative objects. Most prior work leverages the disturbance to the wireless signals for monitoring the intruding object. Youssef et al. demonstrate the DfP feasibility and raise its essential challenges [26]. Xu *et al*. propose an active node based method to use the disturbance from the human body to the RF pattern for indoor localization [27]. A following work SCPL is proposed to model the human trajectory through Viterbi algorithm [6]. Compared to our work, these two works use much powerful active tags and unlicensed RF bands. Meanwhile, the location accuracy of SCPL is 1.3 m, lower than Twins based tracking scheme. Although the work [8] has an accurate detection rate, the system utilize active tags, which may introduce a high cost in large scale applications. TASA [7] provides the function of tag-free activity sensing or route tracking. TASA also exploit the RSS change for motion detection. TASA, however, still needs to involve active tags for reliable sensitivity in the activity sensing. Differing from these previous device-free works, Twins is solely based on passive tags, which is more cost-effective. Meanwhile, Twins is a novel detecting method that first leverages the critical state phenomenon of coupling tags.

It has been observed that nearby tags can produce interference to each other. Weigand and Dobkin conduct experiments over two tag arrays at two planes [14]. The result reported in [14] shows that the successful interrogation rate of tags is severely affected when two parallel arrays are approaching to each other. Later, Chen *et al*. propose a model for nearby tags to formulate their interference affect [13].

IX. Conclusion

In this paper, we propose a novel device-free object tracking scheme, Twins. We contribute to both the theory and practice of a new observed phenomenon, i.e., critical state on two adjacent tags. We also design a practical tracking method using passive tags. The extensive real experiments demonstrate the

effectiveness of our method. Our future work includes studying critical state on a single tag, utilizing Twins to track multiple objects, and extending the detection region by refining the tracking algorithms.

X. ACKNOWLEDGEMENTS

This work was supported in part by National Basic Research Program of China (973 Program) under Grant No. 2015CB351705, NSFC under Grant No. 61325013, 61190112, 61373175, 61172090, and 61402359; the Natural Science Basic Research Plan in Shaanxi Province of China under Grant No. 2014JQ832; the Specialized Research Fund for the Doctoral Program of Higher Education under Grant No. 20130201120016; the Fundamental Research Funds for the Central Universities under Grant No. XJJ2014049 and XKJC2014008. Chen Qian is supported by University of Kentucky Faculty Startup Grant and National Science Foundation grant CNS-1464335. Wei Xi is the corresponding author.

REFERENCES

[1] X. Zhu, Q. Li, and G. Chen, "APT: Accurate Outdoor Pedestrian Tracking with Smartphones," in Proceedings of IEEE INFOCOM, 2013.

[2] S. Guha, K. Plarre, D. Lissner, S. Mitra, and B. Krishna, "AutoWitness: Locating and Tracking Stolen Property While Tolerating GPS and Radio Outages," in Proceedings of ACM SenSys, 2010.

[3] L. M. Ni, Y. Liu, Y. C. Lau, and A. Patil, "LANDMARC: Indoor Location Sensing Using Active RFID," ACM Wireless Networks, (WINET), vol. 10, iss. 6, pp. 701-710, 2004.

[4] J. Wang, F. Adib, R. Knepper, D. Katabi, and D. Rus, "RF-Compass: Robot Object Manipulation using RFIDs," in Proceedings of ACM MobiCom, 2013.

[5] J. Maneesilp, C. Wang, H. Wu, and N.-F. Tzeng, "RFID Support for Accurate 3D Localization," IEEE Transactions on Computers, vol. 62, iss. 7, pp. 1447-1459, 2013.

[6] C. Xu, B. Firner, R. S. Moore, Y. Zhang, W. Trappe, R. Howard, F. Zhang, and N. An, "Scpl: Indoor Device-free Multi-subject Counting and Localization using Radio Signal Strength," in Proceedings of ACM IPSN, 2013.

[7] D. Zhang, J. Zhou, M. Guo, J. Cao, and T. Li, "TASA: Tag-Free Activity Sensing Using RFID Tag Arrays," IEEE Transactions on Parallel and Distributed Systems (TPDS) vol. 22, iss. 4, pp. 558-570, 2011.

[8] Y. Liu, L. Chen, J. Pei, Q. Chen, and Y. Zhao, "Mining Frequent Trajectory Patterns for Activity Monitoring Using Radio Frequency Tag Arrays," in Proceedings of IEEE PerCom, 2007.

[9] L. Yang, Y. Chen, X. yang Li, C. Xiao, M. Li, and Y. Liu, "Tagoram: Real-time Tracking of Mobile RFID Tags to High Precision Using COTS Devices," in Proceedings of ACM MobiCom, 2014.

[10] Y. Liu, Y. He, M. Li, J. Wang, K. Liu, and X. yang. Li, "Does Wireless Sensor Network Scale? A Measurement Study on GreenOrbs", IEEE Transactions on Parallel and Distributed Systems (TPDS), vol. 24, iss. 10, pp. 1983-1993, 2013.

[11] D. M. Dobkin, The RF in RFID, Passive UHF RFID in Practice: Elsevier Inc., 2007.

[12] R. K. Wangsness, Electromagnetic Fields: Wiley-VCH, 1986.

[13] X. Chen, F. Lu, and T. T. Ye, "The "Weak Spots" in Stacked UHF RFID Tags in NFC Applications," in Proceedings of IEEE RFID, 2010.

[14] S. M. Weigand and D. M. Dobkin, "Multiple RFID Tag Plane Array Effects," in Proceedings of IEEE Antennas and Propagation Society International Symposium, 2006.

[15] A.Doucet, N. D. Freitas, and N. J. Gordon, Sequential Monte Carlo Methods in Practice: Springer, 2001.

[16] M. K. Pitt and N. Shephard, "Filtering via Simulation: Auxiliary Particle Filters," Journal of the American Statistical Association, vol. 94, iss. 446, pp. 590-599, 1999.

[17] P. Mohan, V. N. Padmanabhan, and R. Ramjee, "Nericell: Rich Monitoring of Road and Traffic Conditions using Mobile Smartphones," in Proceedings of ACM Sensys, 2008.

[18] J. Xiao, K. Wu, Y. Yi, L. Wang, and L. M. Ni, "Passive Device-free Indoor Localization Using Channel State Information," in Proceedings of the 33rd IEEE International Conference on Distributed Computing Systems (ICDCS), Philadelphia, USA, 2013.

[19] J. Liu, B. Priyantha, T. Hart, H. S. Ramos, A. A. F. Loureiro, and Q. Wang, "Energy Efficient GPS Sensing with Cloud Offloading," in Proceedings of ACM Sensys, 2012.

[20] Y. Chen, D. Lymberopoulos, J. Liu, and B. Priyantha, "Fm-based Indoor Localization," in Proceedings of ACM Mobisys, 2012.

[21] R. Nandakumar, K. Chintalapudi, and V. Padmanabhan, "Centaur: Locating Devices in an Office Environment," in Proceedings of ACM Mobicom, 2012.

[22] A. Rai, K. K. Chintalapudi, V. N. Padmanabhan, and R. Sen, "Zee: Zero-Effort Crowdsourcing for Indoor Localization," in Proceedings of ACM MobiCom, 2012.

[23] Z. Yang, C. Wu, and Y. Liu, "Locating in Fingerprint Space: Wireless Indoor Localization with Little Human Intervention," in Proceedings of ACM MobiCom, 2012.

[24] J. Wang and D. Katabi, "Dude, Where's My Card? RFID Positioning That Works with Multipath and Non-Line of Sight," in Proceedings of ACM Sigcomm, 2013.

[25] J. S. Choi, H. Lee, D. W. Engels, and R. Elmasri, "Passive UHF RFID-Based Localization Using Detection of Tag Interference on Smart Shelf," IEEE TRANSACTIONS ON SYSTEMS, MAN, AND CYBERNETICS—PART C: APPLICATIONS AND REVIEWS, vol. 42, iss. 2, pp. 268-274, 2012.

[26] M. Youssef, M. Mah, and A. Agrawala, "Challenges: Device-free Passive Localization for Wireless Environments," in Proceedings of ACM MobiCom, 2007.

[27] C. Xu, B. Firner, Y. Zhang, R. Howard, and J. Li, "Improving RF-based Device-free Passive Localization in Cluttered Indoor Environments through Probabilistic Classification Methods," in Proceedings of ACM IPSN, 2012.

[28] U. Rueppel, K. Stuebbe, "BIM-Based Indoor Emergency Navigation System for Complex Buildings", Tsinghua Science and Technology, vol. 13, iss. S1, pp. 362-367, 2008.

[29] K. Wu, J. Xiao, Y. Yi, D. Chen, X. Luo, and L. M. Ni, "CSI-based Indoor Localization", , IEEE Transactions on Parallel and Distributed Systems, vol. 24, iss. 7, pp. 1300-1309, 2013.

[30] Z. Yang, Z. Zhou, and Y. Liu, "From RSSI to CSI: Indoor Localization via Channel Response", Journal of ACM Computing Surveys, vol. 46, iss. 2, 2014.

[31] W. Huang, Y. Xiong, X. yang Li, H. Lin, X. Mao, P. Yang, Y. Liu, and X. Wang, "Swadloon: Direction Finding and Indoor Localization Using Acoustic Signal by Shaking Smartphones", IEEE Transaction on Mobile Computing, vol. PP, iss. 99, 2014.

[32] Z. Li, M. Li, J. Wang, and Z. Cao, "Ubiquitous Data Collection for Mobile Users in Wireless Sensor Networks", in Proceedings of IEEE INFOCOM, 2011.

[33] Z. Li, W. Chen, C. Li, M. L, X. yang Li, and Y. Liu, "FLIGHT: Clock Calibration Using Fluorescent Lighting", in Proceedings of ACM MobiCom, 2012.

Jinsong Han (M'04) is currently an associate professor at Xi'an Jiaotong University. He received his Ph.D. degree on Computer Science from Hong Kong University of Science and Technology. His research interests include mobile computing, RFID, and wireless network. He is a member of CCF, ACM, and IEEE.

Chen Qian (M'08) is an Assistant Professor at the Department of Computer Science, University of Kentucky. He received the B.Sc. degree from Nanjing University in 2006, the M.Phil. degree from the Hong Kong University of Science and Technology in 2008, and the Ph.D. degree from the University of Texas at Austin in 2013, all in Computer Science. His research interests include computer networking, data-center networks, software-defined networking, and mobile computing. He is the recipient of the James C. Browne Outstanding Graduate Fellowship in 2011. He is a member of IEEE and ACM.

Xing Wang is a M.D candidate at Xi'an Jiaotong University, Xi'an. Her research interests include RFID, localization, and smart sensing.

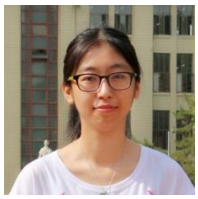

Dan Ma received her MPhil degree from Dept. of Computer Science and Engineering, Xi'an Jiaotong University. Her research interests include RFID, information security, and wireless network.

Jizhong Zhao is a Professor at the Department of Computer Science and Technology, Xi'an Jiaotong University. His research interests include computer software, pervasive computing, distributed systems, network security. He is a member of CCF, ACM, and IEEE.

Wei Xi is a postdoctoral research fellow at Xi'an Jiaotong University. He received his Ph.D degree on Computer Science from Xi'an Jiaotong University in 2014. His research interests include wireless networks, smart sensing, and mobile computing. He is a member of CCF, ACM, and IEEE.

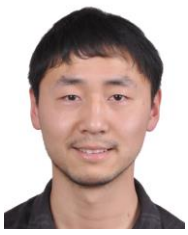

Zhiping Jiang is a Ph.D candidate at Xi'an Jiaotong University, Xi'an. His research interests include localization, smart sensing, wireless communication, and image processing.

Zhi Wang a postdoctoral research fellow at Xi'an Jiaotong University. He received his Ph.D degree on Computer Science from Xi'an Jiaotong University in 2014. His research interests include wireless networks, smart sensing, and mobile computing.